IOPscience iopscience.iop.org

Home Search Collections Journals About Contact us My IOPscience

Analyzing friction forces with the Jarzynski equality

This article has been downloaded from IOPscience. Please scroll down to see the full text article.

2008 J. Phys.: Condens. Matter 20 354008

(http://iopscience.iop.org/0953-8984/20/35/354008)

View the table of contents for this issue, or go to the journal homepage for more

Download details:
IP Address: 129.252.86.83
The article was downloaded on 29/05/2010 at 14:38

Please note that terms and conditions apply.

IOP PUBLISHING JOURNAL OF PHYSICS: CONDENSED MATTER

J. Phys.: Condens. Matter **20** (2008) 354008 (7pp) doi:10.1088/0953-8984/20/35/354008

Analyzing friction forces with the Jarzynski equality

Ronen Berkovich, Joseph Klafter and Michael Urbakh

School of Chemistry, Tel Aviv University, 69978 Tel Aviv, Israel

Received 4 March 2008, in final form 18 April 2008
Published 11 August 2008
Online at stacks.iop.org/JPhysCM/20/354008

Abstract

We investigate the applicability of the Jarzynski equality for reconstructing the energy landscape from force measurements obtained in single molecular unbinding and friction experiments. We demonstrate that single-well molecular potentials, such as the Lennard-Jones potential, could be accurately recovered using a reasonable number of force traces (∼100) obtained for velocities which are experimentally accessible, $v \approx 5$–100 nm s^{-1}. The situation becomes more complex in the presence of potential barriers in the energy profile. These include the double-well and periodic potentials that we consider here. The slow convergence of the reconstruction procedure results from a large energy dissipation which occurs during jumps across the potential barriers. We suggest a modification of the reconstruction procedure which allows the recovering of the correct shape of the potential wells even in the presence of potential barriers. However, a reconstruction of the potential shape in the vicinity of potential maxima requires additional information.

(Some figures in this article are in colour only in the electronic version)

1. Introduction

Experiments that probe mechanical forces on small scales provide a versatile tool for studying molecular adhesion and friction through the response to the mechanical stress of single molecules or of nanoscale tips. The probing techniques include atomic force microscopy (AFM) [1, 2], biomembrane force probe microscopy [3] and optical tweezers [4, 5]. Examples of processes that are investigated are the specific binding of ligand-receptor [6, 7], protein unfolding [8, 9], the mechanical properties of single polymer molecules such as RNA [10, 11] and friction on the atomic scale [1, 2]. In these experiments, one probes forces along a reaction coordinate. One of the main objectives of the force measurements is to get information on the free-energy landscape of the system under investigation. In friction force measurements this aim is usually approached by comparing the force time series measured in the stick–slip regime of motion with the results of calculations within Tomlinson-like models [12–14], which provides an estimation of the amplitude of surface potential corrugation. However, this procedure is not unique and it does not give detailed information on the surface potential. Additional complications arise from the fact that the results of calculations depend on the value of the viscous dissipation constant entering the model, which is also unknown.

Recently, another approach for determining an energy landscape from force measurements has attracted a lot of attention, mainly within the framework of single-molecular force measurements [5, 15–18]. In these experiments, one measures the spring force, F, versus time or extension, and unbinding and rebinding events can be identified by the kinks in the corresponding force traces. A way to relate the free-energy difference between two thermodynamic states, ΔG, to the work, w_t, performed in converting one state to another is through the Jarzynski equality (JE) [15],

$$e^{-\beta \Delta G(z)} = \langle e^{-\beta w_t} \rangle \tag{1}$$

where $\beta = 1/kT$, k is *Boltzmann's* constant, T is the absolute temperature and $\langle \cdots \rangle$ denotes the ensemble's average. The equality allows us to extract equilibrium information from nonequilibrium measurements—getting static internal information on the system from its dynamics. The accumulated work can be found as a path integral of the measured or calculated force over the reaction coordinate. JE has been applied to reconstruct the free energy of a pulled substance from experimentally measured [5, 8, 18] and numerically simulated [17, 19–23] force traces, in single molecular force spectroscopy.

However, so far this approach was not applied to the interpretation of friction force measurements. In this work we

 © 2008 IOP Publishing Ltd Printed in the UK

demonstrate that the use of JE allows us to reconstruct a surface energy profile defined by a periodic potential from the time series of frictional forces.

2. Jarzynski's equality

JE deals with free-energy differences between states described by different values of the coupling parameter λ. In the context of force experiments, it gives the free energy of the entire system at different times. However, the position of the pulling molecule, or tip, fluctuates, and as a result this is not the same as the variation of the free energy along the pulling coordinate, which we are seeking. This problem has been resolved by *Szabo and Hummer*, who presented the JE in the more applicable form [17]:

$$G_0(z) = -\frac{1}{\beta}\ln\left[\frac{\sum_t \left(\frac{\langle\delta(z-z_t)\mathrm{e}^{-\beta w_t}\rangle}{\langle\mathrm{e}^{-\beta w_t}\rangle}\right)}{\sum_t \left(\frac{\mathrm{e}^{-\beta V(z,t)}}{\langle\mathrm{e}^{-\beta w_t}\rangle}\right)}\right] \tag{2}$$

where $V(z,t) = k_\mathrm{s}/2(z(t)-\lambda(t))^2$ is the harmonic potential describing the interaction with the pulling device, k_s is the effective elastic constant of the pulling device (for instance, of the AFM cantilever) and $\lambda(t) = vt$ is the position of the AFM support or of the bead, whichs move with a constant velocity v.

Integrating equation (2) over z gives the Jarzynski equality in equation (1). When putting JE into practice, it is important to emphasize several aspects of this equality that have to be taken into account. The main quantity that JE uses is the averaged weighted work $\langle\mathrm{e}^{-\beta w_t}\rangle$ rather than the work itself. This presents a major difficulty in the practical use of JE, since the exponential average in equation (2) is dominated by the rare events which correspond to small values of the work and emerge from the work probability distribution's tails. For this reason the sampling of those trajectories that hold these rare events is very meaningful [21, 24, 25]. Below, we examine the sampling problem by discussing the required number of realizations for a reasonable convergence of the free energy. Another issue that should be addressed is the dependence of the required number of realizations on the pulling velocity. Due to the sampling problems, the further away our system gets from equilibrium, there will be a price to pay, which is expressed in the statistics.

3. Langevin equation (LE)

In order to illustrate the procedure for reconstruction of the free energy, we generate force time series from the Langevin simulations of single-molecular unbinding and friction. Then the accumulated work can be calculated by a simple integration of the force trajectories:

$$w_t = -\int F(t)\,\mathrm{d}\lambda = -\int F(t)v\,\mathrm{d}t. \tag{3}$$

We start from the one-dimensional Langevin equation of motion for a particle of mass m:

$$m\frac{\mathrm{d}^2z(t)}{\mathrm{d}t^2} = -\varsigma\frac{\mathrm{d}z(t)}{\mathrm{d}t} + \Gamma(t) - \frac{\partial U(z,t)}{\partial z}. \tag{4}$$

Here $z(t)$ is the particle position, $U(z,t)$ is the potential experienced by the particle, ς is the microscopic friction coefficient, which is related to the diffusion coefficient D by $\varsigma = \frac{kT}{D}$, and $\Gamma(t)$ is a fluctuating random force which is characterized by $\langle\Gamma(t)\rangle = 0$ and satisfies the fluctuation-dissipation relation $\langle\Gamma(t)\Gamma(t')\rangle = 2\varsigma kT\delta(t-t')$, where $\delta(t)$ is the Dirac delta function. Due to the stochastic nature of LE we obtain a large number of different trajectories for any given initial condition.

In the case of nanoscale systems considered here, the effect of inertia on the dynamics is usually negligible, and the full Langevin description in equation (4) can be reduced to the over-damped one given by the following equation:

$$\frac{\mathrm{d}z(t)}{\mathrm{d}t} = -\beta D\left(\Gamma(t) - \frac{\partial U(z,t)}{\partial z}\right). \tag{5}$$

In the calculations presented below, we limit ourselves to this equation.

The total potential experienced by the pulled molecule or tip, $U(z)$, includes two contributions: the inherent potential of the system under study, $\Phi(z)$, and the potential describing the interaction with the pulling device, $V(z,t)$. In the case of unbinding or unfolding of single molecules the potential $\Phi(z)$ defines the potential energy landscape of the molecule, while in the framework of friction $\Phi(z)$ is a periodic potential which describes an interaction between the driven tip and the substrate. The force measured in the unbinding and friction experiments is given by

$$F(t) = -k_\mathrm{s}(z(t) - vt). \tag{6}$$

4. Lennard-Jones potential

In order to demonstrate how the JE works, we start from the case of the rupture of molecular bonds. Here the potential $\Phi(z)$ that is chosen is the *Lennard-Jones* potential

$$\Phi_\mathrm{LJ}(z) = U_0\left[\left(\frac{\sigma}{z}\right)^{12} - 2\left(\frac{\sigma}{z}\right)^{6}\right] \tag{7}$$

where U_0 is the depth of the potential well and σ is the position of the potential minima. Figure 1 presents an example of the force time series obtained from a numerical solution of the Langevin equation (5) with the potential in (7).

The rupture force is quantified by the maximum extension of the spring, which is followed by rapid recoil to its rest position. This behavior resembles the stick-to-slip transition in studies on friction [1, 2]. Rupture of the molecular bonds occurs by means of thermally assisted escape from the bound state across an activation barrier. The latter diminishes as the applied force increases, so the rupture force is determined by interplay between the rate of escape in the absence of the external force and the pulling velocity (loading rate) [26, 27]. Thus, the measured forces are not an intrinsic property of the bound complex, but rather depend on the mechanical setup and loading rate applied to the system.

In order to extract the molecular information from the force measurements we collected a number of force

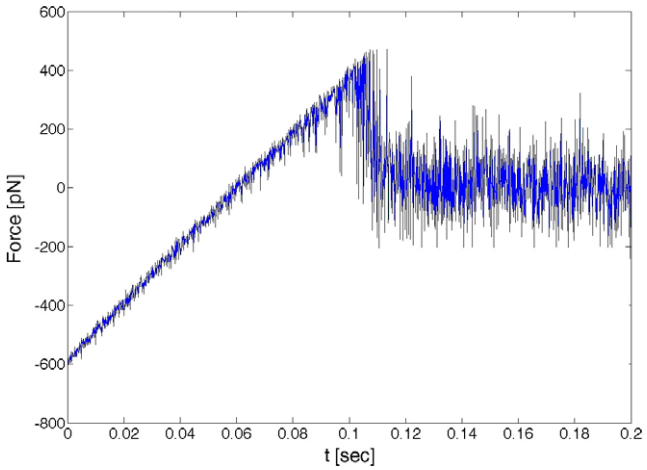

Figure 1. Force time series obtained from the solution of the Langevin equation using the Lennard-Jones potential with $U_0 = 61.5$ pN* nm (∼15 kT), $\sigma = 0.3$ nm, $v = 5$ nm s^{-1}, $T = 300$ K, $D = 530$ nm^2 s^{-1} and $k_s = 2$ N m^{-1}.

trajectories, which are similar to that shown in figure 1 and used in JE (2). The important difference between the original JE (1) and equation (2) used in our calculation is the presence of the delta function, $\delta(z - z_t)$, which allows us to determine the potential from the trajectories z_t. This is done by collecting the weighted work histograms with z-position intervals, and averaging them while reducing the elastic term, as described in (2). The results of the potential reconstruction obtained for different numbers of trajectories are shown in figure 2.

One can see that already ten trajectories may be sufficient for an accurate reconstruction of the lower part of the potential well which is located at $z - \sigma < z_c$, where z_c is the inflection point of the potential profile that corresponds to the maximal value of the unbinding force, $F_{max} = \max\{-d\Phi(z)/dz\}$ for $z > \sigma$. However, in order to achieve an accurate reconstruction of the potential above the inflection point, one needs much better statistics. This is explained by the fact that, for the vast majority of the unbinding events, the molecule escapes from the potential well already under the forces which are smaller than F_{max} and, as a result, the region above the inflection point is probed by rare events only. Simulations of friction measurements, which are presented below, demonstrate that this difficulty presents the major problem for the reconstruction of a surface potential from the friction force traces. Our calculations with the Lennard-Jones potential show that, for the low pulling velocity $v = 5$ nm s^{-1}, the use of a hundred trajectories allows complete reconstruction of the potential (see figure 2(b)). The calculations performed with 1000 trajectories do not show any improvement. Figure 2(c) demonstrates that, as expected, the accuracy of the potential reconstruction decreases with an increase in pulling velocity.

5. Double-well potential

Before discussing the application of JE for reconstructing a periodic potential, let us look at an example of a double-well potential, $\Phi_{DW}(z)$, which has already been considered within

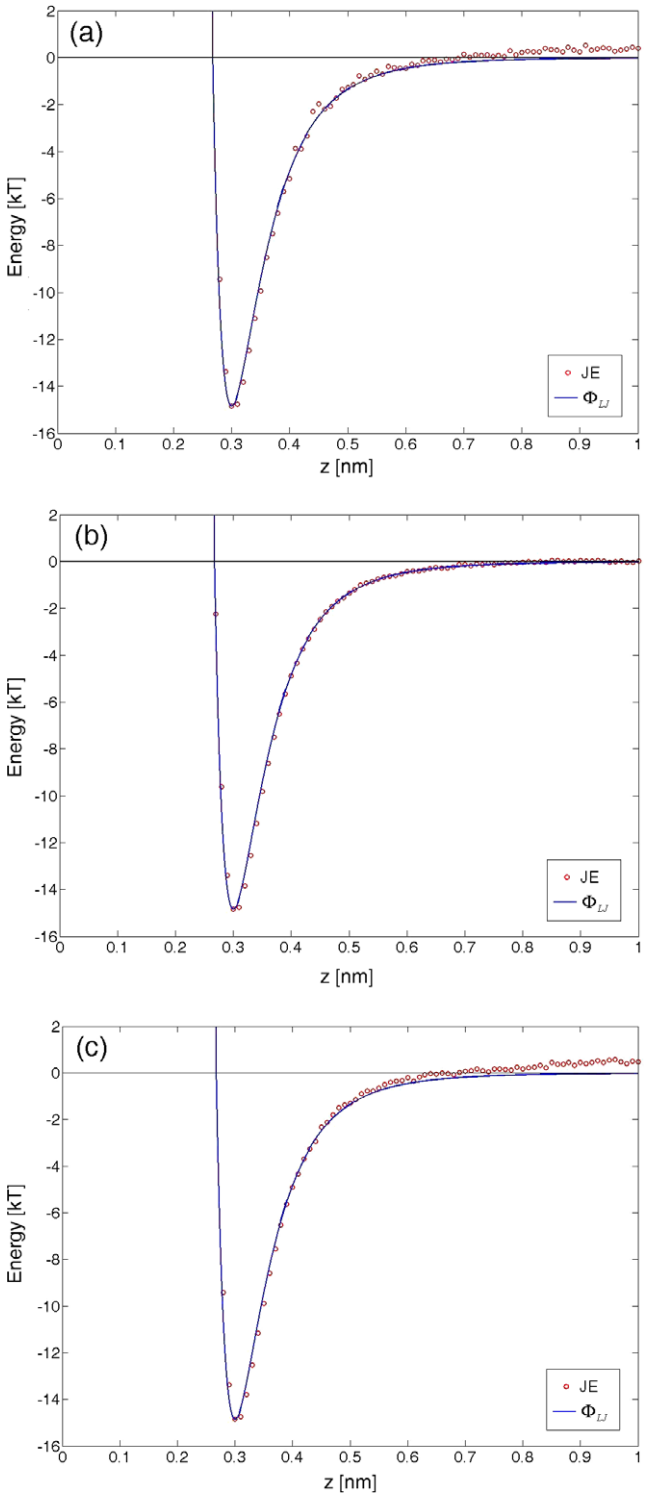

Figure 2. Reconstruction of potential from N pulling trajectories calculated for the Lennard-Jones potential. The solid line (blue online) and the circles (red online) show the reference Lennard-Jones potential given by equation (7) and the results of reconstruction according to equation (2), respectively: (a) number of trajectories, $N = 10$ and the pulling velocity, $v = 5$ nm s^{-1}; (b) $N = 100$ and $v = 5$ nm s^{-1}; (c) $N = 100$ and $v = 500$ nm s^{-1}; other parameters as in figure 1.

the framework of single-molecular unbinding studies [28]:

$$\Phi_{DW}(z) = (a_3 z^3 + a_2 z^2 + a_1 z + a_0)z. \quad (8)$$

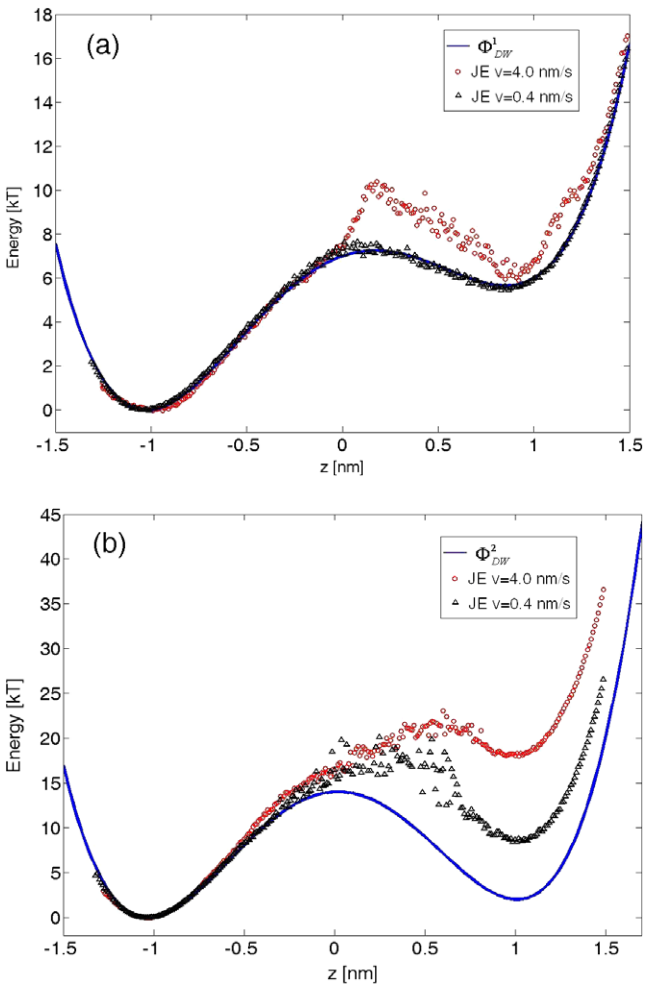

Figure 3. Reconstruction of the double-well potential from 100 pulling trajectories. The solid line (blue online), circles (red online) and triangles (black online) show the reference potential given by equation (8) and the results of reconstruction according to equation (2) obtained for two pulling velocities, $v = 4$ nm s^{-1} and 0.4 nm s^{-1}, respectively: (a) $\Phi^1_{\rm DW}(z) = (5z^3 - 9z^2 + 3)z$, which gives a barrier height of ∼7 kT, and the energy of the second well's minima of ∼6 kT; (b) $\Phi^2_{\rm DW}(z) = (12z^3 - 25z^2 + 1)z$ which gives a barrier height of ∼15 kT, and the energy of the second well's minima of ∼2 kT. The spring constant, $k_{\rm s}$ was taken as 15 pN nm^{-1} and the diffusion coefficient, D, was taken as 1 nm^2 s^{-1}. Energies are in units of kT.

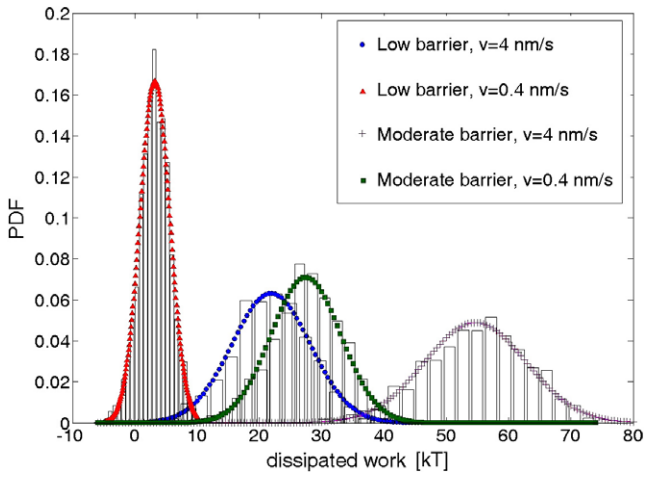

Figure 4. PDFs of the work dissipated during forward and backward cycles for double-well potentials with low and moderate barriers: $\Phi^1_{\rm DW}(z) = (5z^3 - 9z^2 + 3)z$ and $\Phi^2_{\rm DW}(z) = (12z^3 - 25z^2 + 1)z$, respectively. The presented results correspond to two pulling velocities, $v = 4$ nm s^{-1} and 0.4 nm s^{-1}. Energies are in units of kT. Other parameters are as in figure 3.

Here, contrary to the Lennard-Jones potential, there is a barrier separating two potential wells characteristic also of a periodic potential. We have performed calculations for two double-well potentials, $\Phi^1_{\rm DW}$ and $\Phi^2_{\rm DW}$, with the corresponding parameters: (i) $a_3 = 5$ kT nm^{-4}, $a_2 = -9$ kT nm^{-3}, $a_1 = 0$, $a_0 = 3$ kT nm^{-1}, and (ii) $a_3 = 12$ kT nm^{-4}, $a_2 = -25$ kT nm^{-3}, $a_1 = 0$, $a_0 = 1$ kT nm^{-1}. These correspond to low and moderate potential barriers (see figure 3). Figure 3 shows the results of applying JE (2) for a reconstruction of the double-well potential obtained for two different pulling velocities.

A comparison of the results presented in figure 3 with those obtained for the Lennard-Jones potential (see figure 2) leads to the following conclusions: (i) in order to recover a potential profile which includes a barrier, one has to use significantly lower pulling velocities than in the case of a single-well potential; (ii) for moderate pulling velocities the presence of the barrier leads to an increased error in the reconstructed potential as one drives the system further away from its original equilibrium state; and (iii) the error grows with the height of the barrier separating the two wells. The slow convergence of the reconstruction procedure originates from strong energy dissipation during jumps across the potential barrier [25]. The energy dissipation reduces only slowly with a decrease in the pulling velocity; as a result, even for low velocities the system is far from the equilibrium.

Figure 4 shows the probability distribution functions (pdfs) for the energy dissipated during unbinding–rebinding cycles, $W_{\rm d}$, which have been calculated for two kind of the double-well potentials discussed above. We see that for both potentials the most probable dissipated energy and the width of pdfs reduce with a decrease of the pulling velocity. In the case of the moderate potential barrier of 15 kT even for a very low pulling velocity, $v = 0.4$ nm s^{-1}, the most probable dissipated energy is of the order of 30 kT, indicating that the force 'measurements' are performed far from the equilibrium. This is different from the system with the low barrier (∼7 kT), where for $v = 0.4$ nm s^{-1} the most probable dissipated energy becomes as small as 3 kT. As a result the reconstruction procedure is successfully employed for the low potential barrier and requires a very large number of trajectories for the moderate barrier height.

6. Periodic potential

Let us look at experiments where the tip of the friction force microscope (FFM) is dragged along a substrate surface, and the measured lateral force exhibits stick–slip motion, as shown in figure 5. In this case, force traces include many unbinding

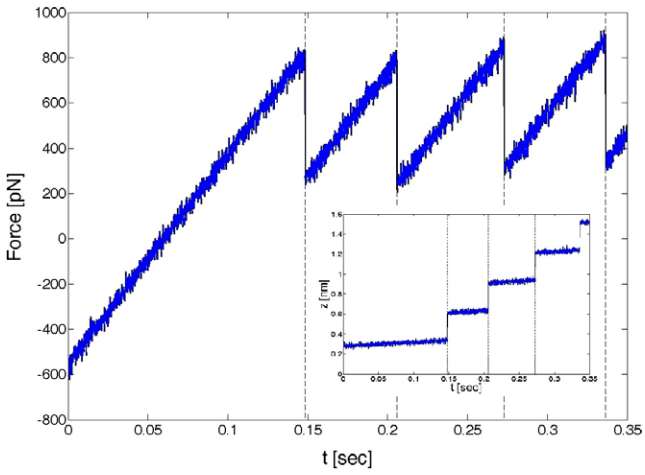

Figure 5. Force time series calculated for the periodic potential given by equation (2). The inset shows the corresponding tip displacement versus time, as obtained by the solution of equation (5) with the periodic potential in equation (9) with $g = 0.3$ nm, and the rest of the parameters are as used earlier in figure 1.

kinks. The results presented in this figure show one of the force traces obtained from the solution of the Langevin equation (5) with the symmetric periodic potential

$$\Phi_{\mathrm{PS}}(z) = -U_0 \cos\left(\frac{2\pi z}{g}\right) \tag{9}$$

where U_0 is the amplitude of the potential corrugation and g is the lattice constant. Stick–slip motion is observed when the pulling spring constant is weaker than the effective stiffness of the surface potential, $\max\{\Phi''(x)\}$. Usually, this condition is written in terms of the Tomlinson parameter, η [29],

$$\eta = \frac{(2\pi)^2 U_0}{k_s g^2} > 1 \tag{10}$$

which in our case equals $\eta = 6.74$.

A direct application of JE (2) to the reconstruction of a potential with a number of barriers, as in the case of a periodic potential, is not quite practical, since it requires a very large number of force traces. As we have already noted above, the slow convergence of the reconstruction procedure originates from strong energy dissipation during slip events when the tip crosses the potential barriers [25, 28]. In order to improve the convergence of reconstructing the potential, we divided the force time series into time segments corresponding to the locations of the tip in the wells along the surface potential. The boundaries between the segments, which are shown by dashed lines in figure 5, have been chosen at those time points where the absolute values of the force derivative are maximal. These points correspond to the jumps (slips) of the tip to the next potential well. Each time segment was treated separately, setting the work accumulated at the previous segment to zero. The surface potential was then obtained using the JE (2) in the same way as described above for the Lennard-Jones potential. Small uncertainties in the determination of the boundaries, which may arise from the limited experimental resolution, do not influence the results. The proposed procedure is justified for relatively low pulling velocities when, after each slip event, the tip approaches the equilibrium state before being pulled out of the well. This means that the rate of relaxation, $\frac{(2\pi)^2 U_0}{g^2 \eta}$, should be higher than the washboard frequency v/g. For the parameters used here this condition is valid for $v < 1200$ nm s^{-1}. For an ideal surface it is enough to reconstruct a potential with one well of the lattice. In order to do this, one needs only one segment of the stick–slip traces. However, in reality there might be defects present at the surface and, in order to identify them and their accurate location and to characterize their potential, we have to analyze a number of stick–slip events.

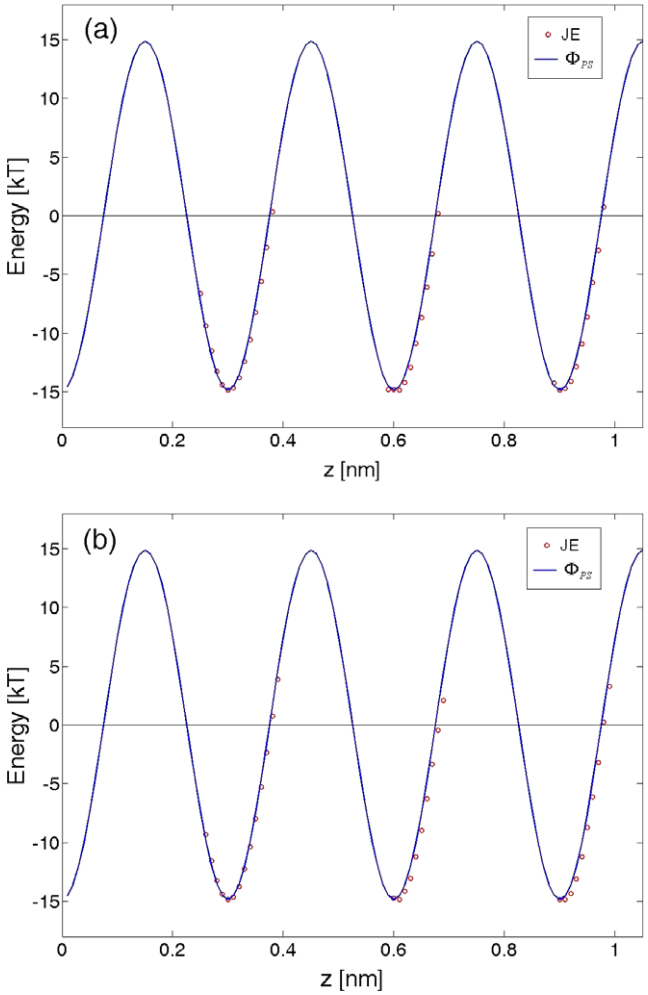

Figure 6. Reconstruction of the symmetric periodic potential from a set of 100 trajectories calculated for the pulling velocities $v = 5$ nm s^{-1} (a) and 500 nm s^{-1} (b). The solid line (blue online) and shows the reference periodic potential given by equation (9). The circles (red online) correspond to the reconstructed potential after filtering as discussed in the text. Other parameters are as in figure 1.

Figure 6 shows the results of the potential reconstruction obtained from 100 force time series which have been calculated for two pulling velocities, $v = 5$ and 500 nm s^{-1}. As in the case of the Lennard-Jones potential, the lower part of the periodic potential (below inflection points) is well reproduced for both velocities. Due to very fast slips of the tip over the

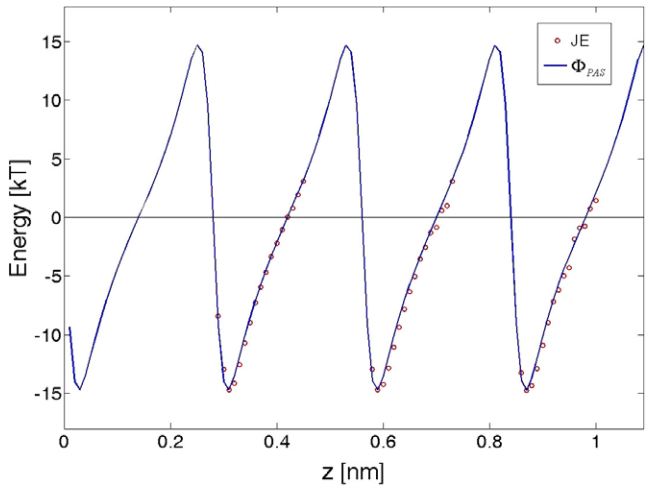

Figure 7. Reconstruction of the asymmetric periodic potential from a set of 100 trajectories calculated for the pulling velocities $v = 5$ nm s^{-1}. The solid line (blue online) and the circles (red online) show the reference periodic potential given by equation (11) and the results of reconstruction after filtering, respectively. Other parameters as in figure 5.

potential barriers, the downhill slopes are not sampled and cannot be recovered.

It should be noted that independent treatment of different time segments of the force time series leads to some complications. Namely, we recover the correct shape of the potential wells but the location of the minima on the energy scale is difficult to determine. We used the following protocol. (i) the tip position is assumed to start from the local equilibrium at each time segment, which corresponds, on average, to the potential minimum. Therefore, except for the first well, we have the same initial conditions, and as a result the minima of the recovered wells lie on the same baseline. In figure 6 the first well was aligned arbitrarily. (ii) We used a filtering procedure according to which we divided the tip extension coordinate into intervals and did not included the contribution of those intervals that were undersampled (due to too short residence time of the tip). Such filtering depends, of course, on the pulling velocity.

In order to demonstrate that the proposed procedure works also for more complex periodic potentials, we consider below an asymmetric periodic potential (see figure 7) described by the following equation [30],

$$\Phi_{\mathrm{PAS}}(z) = -U_0 \frac{ab \sin(\frac{\pi}{g}z)\cos(\frac{\pi}{g}z)}{1 + b\cos^2(\frac{\pi}{g}z)} \qquad (11)$$

where we assumed $a = -0.1$ and $b = -0.9$. Figure 7 shows the potential which has been reconstructed from a hundred force traces calculated for the pulling velocity $v = 5$ nm s^{-1}. It should be noted that a comparison of the friction traces with predictions of Tomlinson-like models gives an estimation for the amplitude of the potential corrugation but does not provide information on the asymmetry of the potential.

7. Conclusions

We have tested the applicability of JE for a reconstruction of the energy landscape from force measurements in single molecular unbinding and friction experiments. We have demonstrated that single-well molecular potentials (for instance, the Lennard-Jones potential) could be accurately recovered using a reasonable number of force traces (∼100) obtained for accessible experimentally velocities ($v \approx$ 5–100 nm s^{-1}). The situation becomes more complex in the presence of potential barriers in the energy profile. As an example, here we considered double-well and periodic potentials. We have found that for moderate or high potential barriers (height $\geqslant$10 kT) a direct application of JE leads to significant errors in the reconstructed potential, even for pulling velocities as low as $v \approx 5$ nm s^{-1}, and a large number of trajectories. The slow convergence of the reconstruction procedure results from a large energy dissipation which occurs during jumps across the potential barriers. We have suggested a modification of the reconstruction procedure which allows the recovering of the correct shape of the potential wells even in the presence of potential barriers. However, a reconstruction of the potential shape in the vicinity of potential maxima requires additional information. An improved potential reconstruction can probably be obtained if one could vary the pulling velocity along the trajectory, allowing for lower velocities near potential barriers.

Acknowledgments

The authors are thankful to Z Tshiprut for useful discussions and acknowledge the support of the German Research Foundation via Grant Ha no. 1517/26-1-3. MU acknowledges the support of the Israel Science Foundation (grant no. 1116/05).

References

[1] Mate C M, McClelland G M, Erlandsson R and Chiang S 1987 *Phys. Rev. Lett.* **59** 1942
[2] Gnecco E, Bennewitz R, Gyalog T, Loppacher C, Bammerlin M, Meyer E and Guntherodt H J 2000 *Phys. Rev. Lett.* **84** 1172
[3] Merkel R, Nassoy P, Leung A, Ritchie K and Evans E 1999 *Nature* **397** 50
[4] Mehta A D, Rief M, Spudich J A, Smith D A and Simmons R M 1999 *Science* **283** 1689
[5] Liphardt J, Dumont S, Smith S B, Tinoco I Jr and Bustamante C 2002 *Science* **296** 1832
[6] Florin E L, Moy V T and Gaub H E 1994 *Science* **264** 415
[7] Nevo R, Stroh C, Kleinberger F, Kaftan D, Brumfeld V, Elbaum M, Reich Z and Hinterdorfer P 2003 *Nat. Struct. Biol.* **10** 553
[8] Oesterhelt F, Oesterhelt D, Pfeiffer M, Engel A, Gaub H E and Muller D J 2000 *Science* **288** 143
[9] Brujic J, Hermans Z R I, Walter K A and Fernandez J M 2006 *Nat. Phys.* **2** 282
[10] Cui Y and Bustamante C 2000 *Proc. Natl Acad. Sci.* **97** 127
[11] Manosas M and Ritort F 2005 *Biophys. J.* **88** 3224
[12] Muser M H, Urbakh M and Robbins M O 2003 *Adv. Chem. Phys.* **126** 187

[13] Dudko O K, Filippov A E, Klafter J and Urbakh M 2002 *Chem. Phys. Lett.* **352** 499
[14] Urbakh M, Klafter J, Gourdon D and Israelachvili J 2004 *Nature* **430** 525
[15] Jarzynski C 1997 *Phys. Rev. Lett.* **78** 2690
[16] Jarzynski C 1997 *Phys. Rev.* E **56** 5018
[17] Hummer G and Szabo A 2001 *Proc. Natl Acad. Sci.* **98** 3658
[18] Harris N C, Song Y and Kiang C H 2007 *Phys. Rev. Lett.* **99** 068101
[19] Kreuzer H J, Payne S H and Livadaru L 2001 *Biophys. J.* **80** 2505
[20] Braun O, Hanke A and Seifert U 2004 *Phys. Rev. Lett.* **93** 158105
[21] Park S and Schulten K 2004 *J. Chem. Phys.* **120** 5946
[22] Minh D D L 2006 *Phys. Rev.* E **74** 061120
[23] Imparato A and Peliti L 2006 *J. Stat. Mech.* P03005
[24] Hummer G 2001 *J. Chem. Phys.* **114** 7330
[25] Jarzynski C 2006 *Phys. Rev.* E **73** 046105
[26] Evans e 2001 *Annu. Rev. Biophys. Biomol. Struct.* **30** 105
[27] Dudko O K, Filippov A E, Klafter J and Urbakh M 2003 *Proc. Natl Acad. Sci.* **100** 11378
[28] Adib A B and Minh D D L 2008 *Phys. Rev. Lett.* **100** 180602
[29] Socoliuc A, Bennewitz R, Gnecco E and Meyer E 2004 *Phys. Rev. Lett.* **92** 134301
[30] Pesz K, Gabrys B J and Bartkiewicz S J 2002 *Phys. Rev.* E **66** 061103